Experimental investigations on a common centrifugal pump operating under gas entrainment conditions

Schäfer, T.; Neumann, M.; Bieberle, A.; Hampel, U.;

Originally published:

March 2017

Nuclear Engineering and Design 316(2017), 1-8

DOI: https://doi.org/10.1016/j.nucengdes.2017.02.035

Experimental investigations on a common centrifugal pump operating under gas entrainment conditions

Thomas Schäfer[1,*], Martin Neumann[2], André Bieberle[1], Uwe Hampel[1,2]

[1] Helmholtz-Zentrum Dresden-Rossendorf, Institute of Fluid Dynamics, Germany

[2] Technische Universität Dresden, AREVA Endowed Chair of Imaging Techniques in Energy and Process Engineering, Germany

*Corresponding author: (thomas.schaefer@hzdr.de)

Abstract

This paper presents an experimental study on the effects of additional gas entrainment in centrifugal pumps designed for conveying liquid phases only. The pump performance has been evaluated for several gas entrainment conditions, and for various operational settings of the pump, such as its alignment and the rotational speed of the impeller. As a main performance indicator the impact of entrained gas on the hydraulic power of the pump has been analyzed using experimental data. Additionally, high-resolution gamma-ray computed tomography (HireCT) operated in time-averaged rotation-synchronized scanning mode has been applied to quantify local phase fraction distributions inside the rapidly rotating pump impeller. Based on these quantitative tomographic measurements, gas holdup profiles along selected streamlines have been calculated and gas accumulation areas inside the impeller chambers have been visualized. Thus, various internally accumulated gas holdup patterns have been identified and, eventually, associated with characteristic pump performance behaviors. Moreover, the tomographic measuring method allowed an enhanced gas holdup analysis in specified pump compartments. As a result, the related specific gas and liquid phase holdup profiles have been evaluated.

Keywords: centrifugal pump, gas entrainment, two-phase flow, gas holdup, gamma-ray computed tomography

1. Introduction

The reliable operation of pumps in power stations is essential for highly available, efficient and safe generation of electricity. For example, in nuclear power stations with light water reactors, emergency core cooling systems are operated with centrifugal pumps. During a

loss-of-coolant accident (LOCA) they continuously convey the coolant to steadily discharge all decay heat produced inside the core. Therefore, coolant is taken from reservoirs, which are, for example, the condensation chambers or the reactor sump. Since the coolant in these reservoirs has free surfaces, gas entrainment due to hollow vortex formation may occur. The vortex formation is initiated by small surface vortices, which are always present in such reservoirs, and can lead to large developed gas entraining hollow vortices (Hecker, 1981). This process depends on various conditions, such as the suction rate of the coolant, the critical submergence of the intake and its geometry, as well as the fluid properties of the coolant (Caruso et al., 2014; Kimura et al., 2008). Gas entrainment into the coolant results in a gas/liquid two-phase flow, which passes the subsequently connected system components of the cooling circuit, like pumps and valves. Preferably, gas entrainment should be avoided, since these system components are usually designed for single-phase liquid flow and the entrained gas may lead to undesired operational states, attended by vibrations and increased mechanical load, which can even damage these components.

In the past, several experimental and numerical studies have been performed, to investigate the operation behavior of centrifugal pumps under various operation conditions. Operation of centrifugal pumps under single-phase flow conditions has been investigated, for example, regarding effects like flow induced pressure pulsations and resulting vibrations and noise (Suhane, 2012) or during start up (Zhang et al., 2013). Furthermore, effects of unsteady flow patterns, resulting from pressure fluctuations, on the pump operation have been analyzed, using numerical models (Gonzales and Santolaria, 2006). Also the influence of the impeller geometries on the hydrodynamics of centrifugal pumps have been numerically investigated and improved designs have been verified (Grapsas et al., 2007; Zhou et al., 2013).

Moreover, observations on centrifugal pumps operating under two-phase flow conditions have been reported. Amongst others, scale model pumps were analyzed in the event of a LOCA by conducting blow down test (Narabayashi et al., 1985) or a full-size nuclear reactor pump was experimentally investigated under high pressure steam/water two-phase flow conditions (Chan et al., 1999). Furthermore, in comparison to experimental results, the gas fraction, pressure and velocity in the impeller of a centrifugal pump were numerically calculated, applying Reynolds-averaged Navier-Stokes equations (Pak and Lee, 1998), or consequences of two-phase flow due to cavitation were identified (Duplaa et al., 2013; Tan et al., 2013; Coutier-Delgosha et al., 2003). Another numerical study was focused on the

influence of bubble diameter and void fraction of entrained gas on the pump operation (Caridad et al., 2008). Recently, the gas accumulation inside a closed impeller of an industrial centrifugal pump under various gas entrainment conditions has been quantified, and corresponding gas holdup areas have been visualized, using high-resolution gamma-ray computed tomography (Schäfer et al., 2015; Neumann et al., 2016).

This study contributes to a better understanding of the impacts of gas entrainment on the performance of centrifugal pumps and provides additional knowledge to operate centrifugal pumps under such conditions or even to improve the pump design correspondingly. Besides, additional datasets are provided for a better modelling of two-phase flows in centrifugal pumps, which may improve future CFD calculations.

2. Materials and methods

In this experimental study a common industrial centrifugal pump (Etachrom BC 032-160/074 C11, KSB) has been investigated, equipped with a closed radial multi vane impeller. The centrifugal pump can be installed either horizontally or vertically, regarding to the impeller orientation, and it is connected to a flow loop, where a defined gas-liquid two-phase flow is circulated by the investigated pump itself. For the experiments, tap water is used as liquid phase and de-oiled pressurized air as gas phase. The liquid is stored in a 600 l reservoir. The liquid flow rate is measured by a magnetic inductive liquid flow meter (MAG 1100, Siemens). The liquid flow meter and a liquid temperature sensor (PT100) are installed upstream of the pump, between the liquid reservoir and an in-house developed gas injection module. Here, gas is injected via four hole-type nozzles, which are uniformly arranged around the circumference of the pipe. The gas injection module is installed at the suction side of the pump and provides an adjustable gas-liquid two-phase flow. The injected gas volume fraction ε_{in} ($0 \leq \varepsilon_{in} < 1$) can be adjusted and the required gas flow rate Q_G is controlled by an air mass flow controller (FMA2600, Omega Newport), which is triggered by a programmable logic controller (SPS-ILC350ETH, Phoenix Contact) considering the current liquid flow rate Q_L according to

$$Q_G = \frac{\varepsilon_{in}}{1-\varepsilon_{in}} \cdot Q_L \,. \tag{1}$$

Optionally, a sophisticated swirl element can be installed inside the gas injection module behind the gas inlet nozzles to adjust the flow regime of the two-phase flow (Figure 1~~Figure 1~~a). Thus, for the experiments, both typical flow regimes, occurring at gas entrainment due to hollow vortex formation, can be provided at the suction side of the pump. These are either a gas-liquid flow with disperse gas phase ("bubbly two-phase flow") (Figure 1~~Figure 1~~b) or a swirling gas-liquid flow with central formed gas core ("swirling two-phase flow") (Figure 1~~Figure 1~~c).

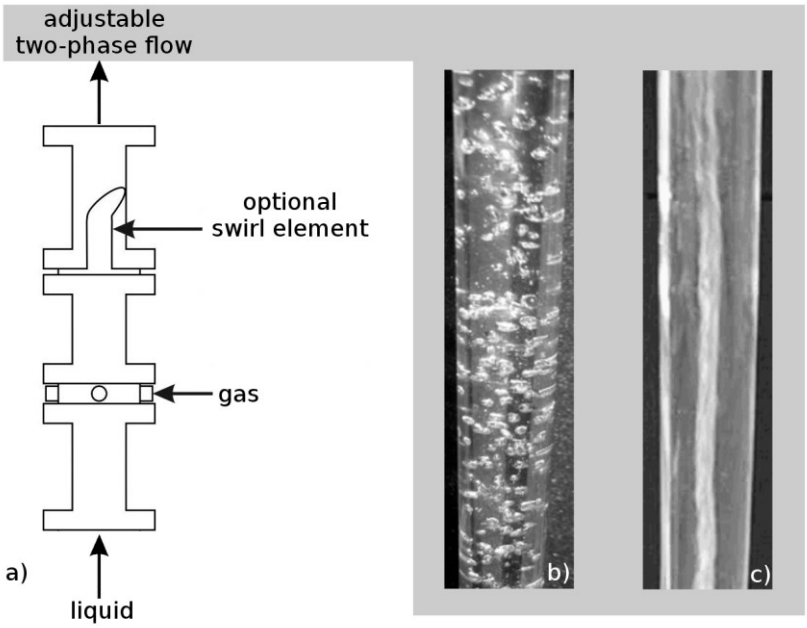

Figure 1: a) Sketch of the multi-mode gas injection module and adjustable flow regimes: b) gas-liquid flow with disperse gas phase ("bubbly two-phase flow") and c) swirling gas-liquid flow with central formed gas core ("swirling two-phase flow").

Furthermore, a heat exchanger (C200 301-1, Funke) in combination with a controlled thermostat (Unistat Tango) is installed in the flow loop at the pressure side of the centrifugal pump to provide a constant liquid temperature of $T = 30°C$ for the experiments. The two-phase flow is conveyed from the gas injection module through the centrifugal pump and the heat exchanger back to the liquid reservoir which acts also as a two-staged separator. Here, the injected gas phase is separated from the liquid phase. Furthermore, the flow loop is instrumented with two pressure sensors to measure the relative pressure at the suction side (PR23, Omega Newport) and the differential pressure across the pump (PD23, Omega Newport).

Additionally, high-resolution gamma-ray computed tomography (HireCT) (Hampel et al. 2007; Bieberle et al., 2012, 2013; Schubert et al., 2011) has been applied to discover the phase distribution inside the operating pump impeller by contactless measurement. The HireCT-system is able to scan objects, which have a maximal diameter of 700 mm. It consists of a temperature stabilized detector arc including 320 scintillation detector elements with a sensitive area of 2 mm x 4 mm and is operated with a collimated isotopic source (^{137}Cs, energy: 662 keV, activity: 180 GBq). The investigated centrifugal pump was placed between the source and the detector arc, which are both fixed on a movable desk.

To resolve the phase fraction distribution inside the fast rotating impeller of the operating pump sharply, tomographic scans are synchronized with the rotational speed of the impeller (Figure 2~~Figure 2~~). Therefore, the rotational speed is measured, using a Hall-effect sensor (GS105502, ZF Electronics). The Hall-effect sensor is placed close to the driving shaft and is connected directly to the HireCT-scanner. This advanced CT measuring method, which is known as time-averaged rotation-synchronized computed tomography, was introduced by (Prasser et al., 2003) for investigations on an axial pump and further developed by (Hampel et al., 2005, 2008; Bieberle et al., 2007).

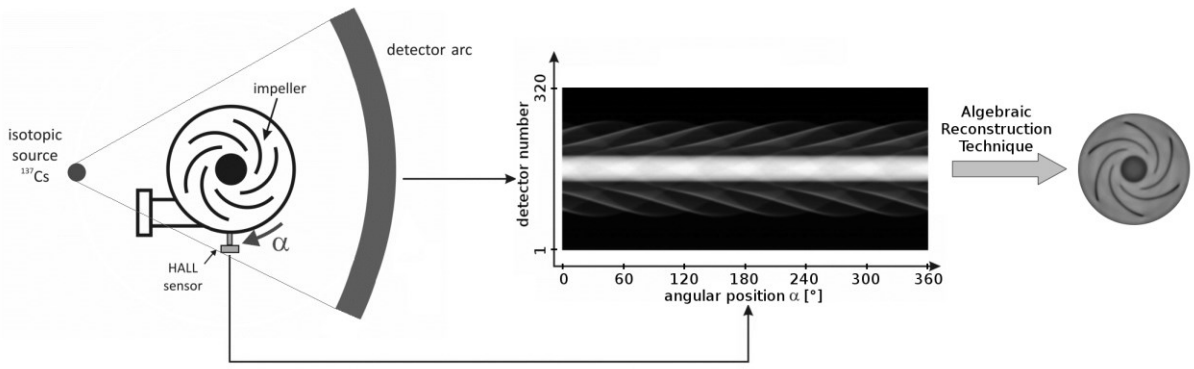

Figure 2: Sketch of HireCT measurement setup (left), data set of measured projections referred to as “sinogram” (middle) and reconstructed attenuation image of the scanned rotating impeller (right).

Applying algebraic reconstruction techniques (ART) (Gordon et al., 1970), non-superimposed cross-sectional images of the attenuation coefficients μ_{ij}, where i and j represent the indices of the image pixels, can be reconstructed from a complete tomographic scan (Figure 2~~Figure 2~~). These images represent the spatial material distribution inside the scanned object, which also includes time-averaged information about the phase fraction distribution

of the conveyed gas-liquid mixture inside the pump. This phase fraction distribution can be visualized and also quantified, by referring the measured distribution of the relative linear attenuation coefficients of the investigated pump under two-phase flow conditions μ_{ij}^{TP} to tomographic scans of defined material distributions (reference states). Thus, the local quantitative gas phase fraction ε_{ij} is calculated according to

$$\varepsilon_{ij} = \frac{\mu_{ij}^{L} - \mu_{ij}^{TP}}{\mu_{ij}^{L} - \mu_{ij}^{G}}, \tag{2}$$

where μ_{ij}^{L} and μ_{ij}^{G} are the spatial distributions of the relative linear attenuation coefficients of the reference states. Here, μ_{ij}^{L} equates to 0% gas (pump completely filled with water) and μ_{ij}^{G} equates to 100% gas (drained pump). The actual spatial resolution of the phase fraction distributions based on the tomographic scans is approximately 2 mm and the measuring uncertainty of the HireCT system regarding the determined quantitative phase fraction values is ≤ ±0.01, which has been proven in a prior study (Bieberle et al., 2015).

3. Results

3.1 Influence of gas entrainment on the pump performance

The performance of the centrifugal pump under gas entrainment conditions is one of the main issues, since the investigated pump was designed for conveying liquids only. Thus, the pump performance at nominal speed (1480 rpm) is experimentally investigated for both pump alignments (horizontal and vertical impeller) and for several gas entrainment conditions. Therefore, the injected gas volume fraction ε_{in} as well as the suction side flow regime ("bubbly two-phase flow" / "swirling two-phase flow") is varied. Based on the associated conveyed liquid flow rates Q_L and the corresponding differential pressures across the pump Δp, the relative hydraulic power is calculated according to

$$P_{hyd,rel}(\varepsilon_{in}) = \frac{P_{hyd}(\varepsilon_{in})}{P_{hyd}(\varepsilon_{in}=0)} = \frac{Q_L(\varepsilon_{in}) \cdot \Delta p(\varepsilon_{in})}{Q_L(\varepsilon_{in}=0) \cdot \Delta p(\varepsilon_{in}=0)}. \tag{3}$$

The resulting performance curves of the pump are shown in Figure 3~~Figure 3~~, where the relative hydraulic power is plotted against the entrained gas volume fraction, depending on the flow regime at the suction side and the alignment of the impeller.

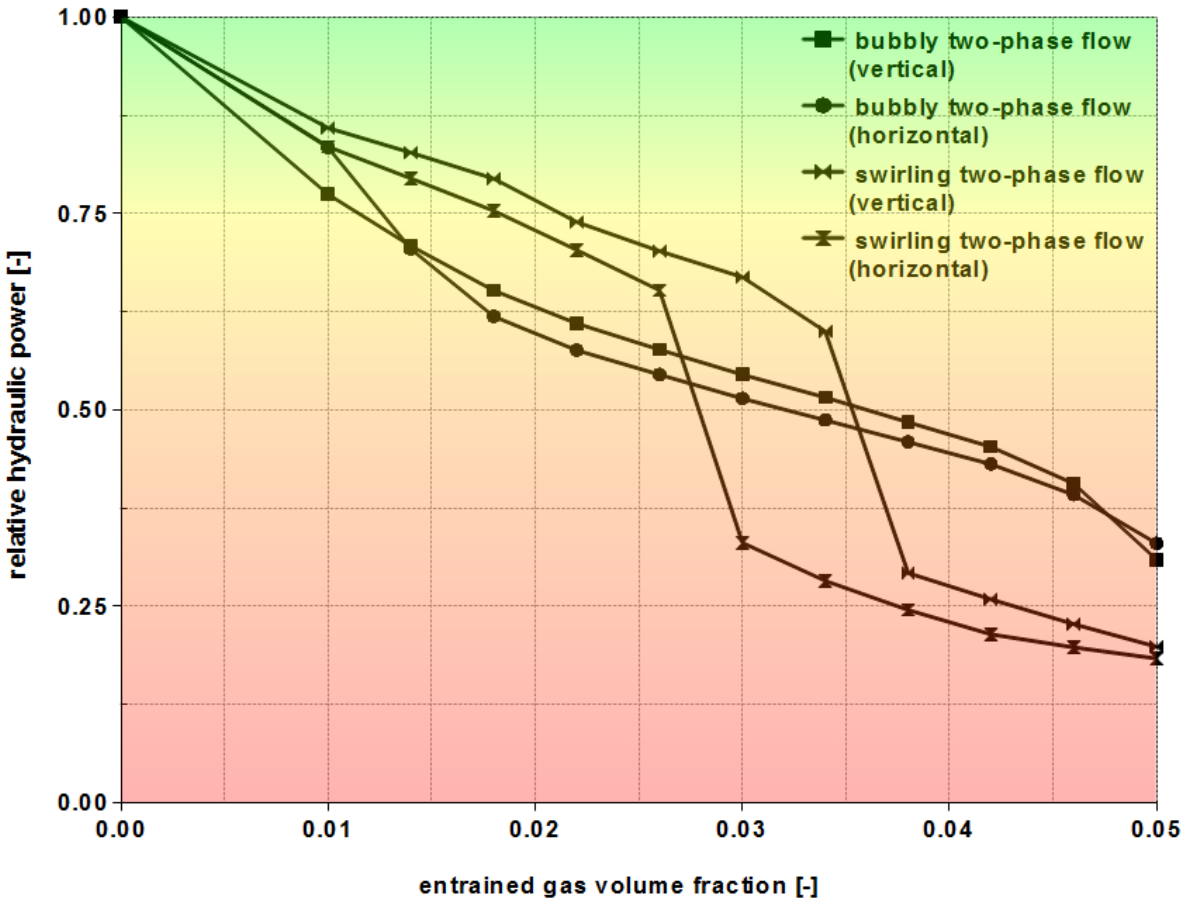

161

162 Figure 3: Performance curves for both installation positions (horizontal and vertical impeller
163 alignment) and various gas entrainment conditions and gas volume fractions.

164 Generally, the relative hydraulic power of the pump decreases with increasing gas
165 entrainment. In case of bubbly two-phase flow the relative hydraulic power decreases
166 continuously, down to nearly 30% of the undisturbed hydraulic power. Here, an almost
167 identical curve was found for both installation positions. This indicates that the impeller
168 alignment has no significant impact on the hydraulic power in case of gas entrainment by
169 bubbly two-phase flow. But in contrast to the continuous decrease of relative hydraulic
170 power at bubbly two-phase flow inlet condition, a remarkable performance discontinuity
171 was observed for both impeller alignments at swirling two-phase flow inlet condition, where
172 the relative hydraulic power decreases steeply down to less than 30%. After that, a further
173 more gently decrease of the relative hydraulic power down to nearly 20% can be observed.
174 Thus, gas entrainment by swirling two-phase flow regime leads to a higher performance
175 drop compared to bubbly two-phase flow regime at same gas volume fraction injection. The
176 observed hydraulic power discontinuity, which is represented by an abrupt performance

drop, occurs at entrained gas volume fractions between $0.026 < \varepsilon_{in} < 0.030$ for the horizontal case, but for the vertical case it happens at slightly higher entrained gas volume fractions between $0.034 < \varepsilon_{in} < 0.038$. Here, the alignment of the impeller wheel has probably a considerable impact.

3.2 Gas holdup accumulation inside the impeller

To study the observed discontinuous performance drop, a set of tomographic scans of the pump with horizontally aligned impeller, operating at 1480rpm, were conducted. The obtained and reconstructed images of the investigated two-phase flow inside the impeller (Figure 4~~Figure 4~~) disclose a remarkable evolution of the phase fraction distribution depending on the entrained gas volume fraction. This is represented in detail in holdup curves, calculated from the tomographic measurement data for three different radially arranged impeller areas. These areas are indicated in Figure 4~~Figure 4~~ and are artificially defined in the measurement plane in radial direction as the inlet area (impeller suction eye, where the fluid enters the impeller), the chamber area (impeller vanes, where the fluid is accelerated) and the outlet area (clearance between the impeller shrouds and the casing, where the fluid is decelerated). Furthermore, the mean value of all curves was calculated and plotted (Figure 4~~Figure 4~~).

Obviously, two states are represented in all holdup curves in the diagram in Figure 4~~Figure 4~~, depending on the entrained gas volume fraction and indicating different flow characteristics inside the pump. They can be assigned to the conditions before and after the performance transition which occurs at entrained gas volume fractions between 0.026 and 0.030 and which was already found in the hydraulic power curve (Figure 3~~Figure 3~~) for the gas entrainment by swirling two-phase flow.

The gas holdup curve of the inlet area (Figure 4~~Figure 4~~) is characterized by a strong linear increase, which can be found at lower entrained gas volume fractions (< 0.018) and indicates a high degree of phase separation and gas accumulation in this area. This is proceeded by a slightly decreasing slope of the holdup curve (at entrained gas volume fractions between 0.018 and 0.026), which indicates a decreasing phase separation of the two-phase flow under this conditions, where more of the entrained gas is conveyed with the liquid. Thus, only a slightly increase of accumulated gas can be found in this impeller area. Here, typical gas holdup values of about 0.2 can be found. Following this, an abrupt holdup drop occurs in

this impeller area at entrained gas volume fractions between 0.026 and 0.030. Now, less phase separation takes place and large amount of prior accumulated gas is displaced by the liquid phase again. This leads to a more homogeneous two-phase flow, which dominates the area again. Consequently, a noticeable drop of accumulated gas holdup down to 0.14 is observable. This reduced holdup value then remains stable, although the entrained gas volume fraction is further increasing.

The gas holdup in the chamber area is also continuously increasing at lower entrained gas volume fractions (< 0.018). Here, nearly the same slew rate as in the inlet area is observable. This indicates again a high phase separation rate, which leads to growing accumulated gas pockets and results in decreasing energy transfer from the impeller blades to the liquid phase. But, in contrast to the inlet area no stagnation or drop of phase separation and lower gas accumulation (saturation) can be found for entrained gas volume fractions between 0.018 and 0.030. During the flow transition (at entrained gas volume fractions between 0.026 and 0.030), also in contrast to the inlet area, the phase separation and thus the gas holdup is increasing very strong. Subsequently, after the transition, only a slightly increasing holdup was detected, which indicates stagnation (saturation) of the gas accumulation capacity in the chamber area under these conditions. While the entrained gas at lower entrained gas volume fractions (≤ 0.026) is exclusively accumulated near to the inlet of the impeller chamber area, there is an appreciable different distribution at higher volume fractions (≥ 0.03). Here, nearly the entire impeller chamber area is filled with gas, which strongly constrains the energy transfer from the impeller blades to the liquid phase, because of losses due to slip between the phases and the compressibility of the gas.

Also, the relative total amount of accumulated gas in the impeller chambers strongly differs for both conditions. While at lower volume fractions about the twelve to fifteen fold of the entrained gas volume fraction is accumulated inside the impeller chamber area, it is much more after the transition. The rapid change of the phase distribution inside the impeller chamber area indicates that the flow regime and thus, the hydrodynamic conditions inside the impeller wheel must have changed rapidly, which leads to more phase separation along the flow inside the chambers. This means, the type of suction side two-phase flow regime has a critical impact on the hydrodynamic conditions inside the impeller wheel and thus, on the performance and reliability of the centrifugal pump.

In the outlet area, in general, only small amounts of accumulated gas can be found and the holdup values are only slightly increasing over the whole range of entrained gas volume fraction, which was chosen for the investigations. However, here also a transition is observable, which is indicated by a very small change of slope after the critical entrained gas volume fraction of 0.03.

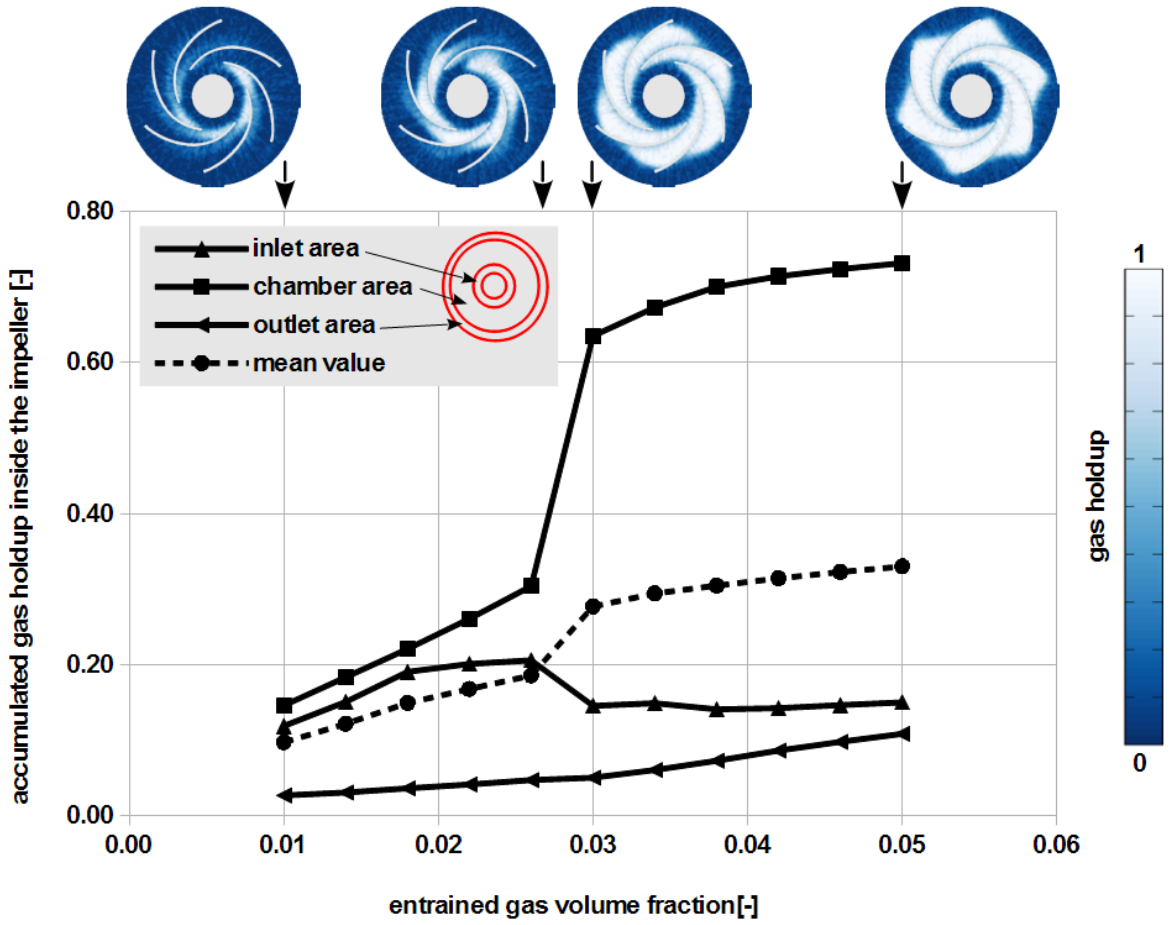

Figure 4: Gas holdup accumulation inside the impeller of an industrial centrifugal pump, operating at 1480 rpm, depending on the entrained gas volume fraction, for horizontal impeller orientation and gas entrainment by swirling two-phase flow with central formed gas core.

3.3 Impact of rotational speed

Furthermore, the effect of rotational speed of the centrifugal pump impeller on the accumulated gas holdup inside the impeller, depending on the impeller orientation and the entrained gas volume fraction, has been investigated for two different gas entrainment conditions. These are gas entrainment by bubbly two-phase flow (Figure 5a) and gas entrainment by swirling two-phase flow (Figure 5b). Therefore, the rotational speed was

varied and the pump was operated, besides nominal speed (1480 rpm), at lower (1300 rpm) and higher (1600 rpm) rotational speed.

It was found that the rotational speed of the impeller has only a very small influence on the amount of accumulated gas inside the impeller chambers if gas is entrained by swirling two-phase flow (Figure 5b). In the case of the vertical alignment of the impeller the gas holdup stays nearly constant over a wide range of rotational speed, while the gas holdup is slightly decreasing if the impeller is horizontally arranged.

If gas entrainment takes place under bubbly two-phase flow conditions (Figure 5a) the rotational speed has a stronger impact on the amount of accumulated gas. Here, with increasing rotational speed the gas holdup is slightly decreasing. This can be explained by a better energy transfer from the impeller blades to the liquid phase of the two-phase flow. While the radial acceleration is increasing at higher rotational speeds, the phase separation of the homogeneous bubbly two-phase flow inside the impeller chambers is constrained. Thus, the present disperse gaseous phase is better carried out from the impeller chamber, together with the liquid. Furthermore, the holdup is decreasing nearly linear with increasing rotational speed, if the impeller wheel is horizontally arranged. This indicates the continuous impact of the rotational speed and therewith the radial acceleration on the two-phase flow, which is, at least for the investigated range of entrained gas in the experiments ($0.01 \leq \varepsilon_{in} \leq 0.05$), independent from the amount of entrained gas. In contrast, deviant, nonlinear behavior was found for the vertical arranged impeller at higher rotational speed (1600 rpm) and for higher gas entrainment rates (gas volume fraction 0.05). For this case a strong decrease of the accumulated gas holdup was observed. This indicates again the positive impact of increasing rotational speed on conveying of bubbly two-phase flow. Thus, independent from the impeller alignment, higher rotational speed results in higher radial acceleration, which is advantageous for steadily conveying of bubbly two-phase flow.

In general it is identifiable, that the amount of accumulated gas inside the impeller chamber depends on the impeller installation orientation. If the impeller is horizontally arranged the gas holdup is always higher (in certain cases even significantly higher) than in the cases where the impeller is vertically arranged. This behavior was found for nearly all investigated operational conditions, except for very small gas entrainment (gas volume fraction 0.01) in combination with very high rotational speeds (1600 rpm), where the accumulated gas

holdup remains nearly on the same level in both installation orientations. This indicates a stable, poorly separated two-phase flow inside the impeller chambers, which allows high conveyability of the two-phase flow.

Furthermore, a strong deviation in the amount of accumulated gas was found, depending on the impeller orientation, for gas entrainment by swirling two-phase flow with formed gas core (Figure 5b) and a gas entrainment volume fraction of 0.03. However, this is caused by the discontinuous flow transition, which was typically found only for gas entrainment by swirling two-phase flow with formed gas core, as already discussed before. Based on the results of the experiments, which are represented in the diagram in Figure 4~~Figure 4~~, it is known that the gas holdup inside the impeller is smaller before the transition takes place and it is much higher after this transition. Since the critical entrained gas volume fraction for this transition is depending on the impeller orientation (Figure 3~~Figure 3~~), it is obvious, that the observed large holdup differences between the horizontal and the vertical case in the diagram in Figure 5b, for the entrained gas volume fraction of 0.03, are caused by this shift of transition.

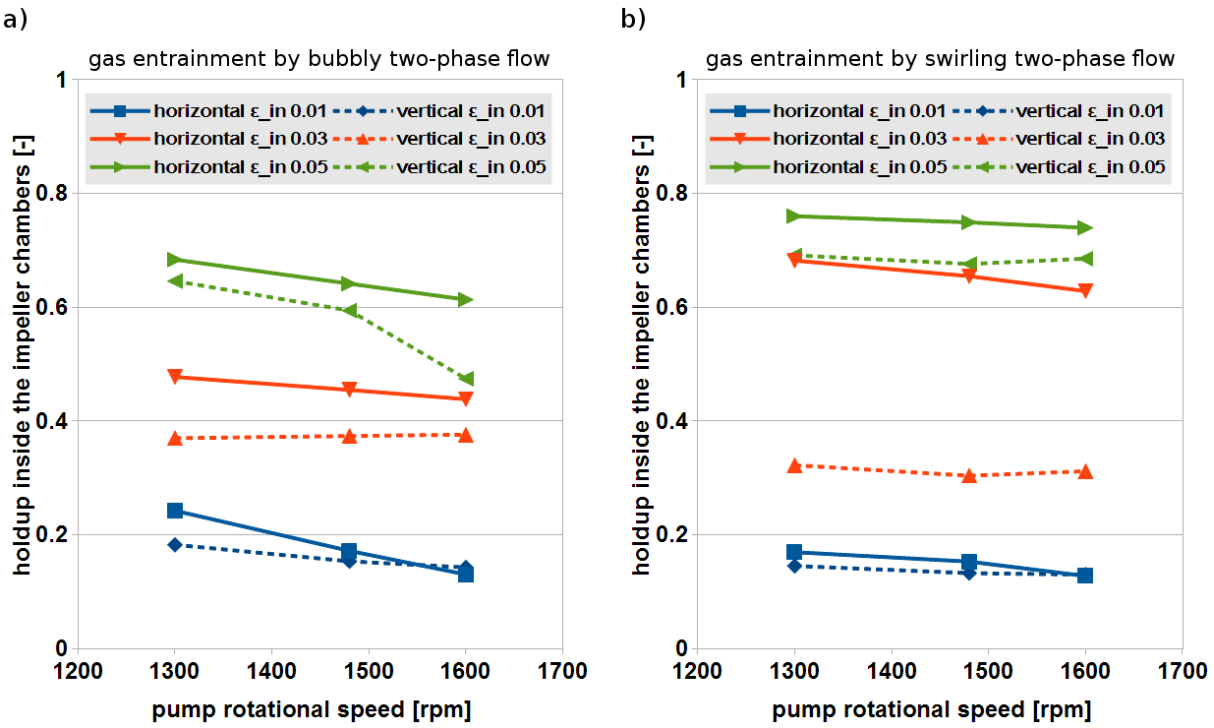

Figure 5: Effect of rotational speed of the centrifugal pump on the gas holdup, depending on the impeller orientation and the entrained gas volume fraction, for gas entrainment by a) bubbly two-phase flow and b) swirling two-phase flow.

3.4 Impact of a balancing hole

The impeller is featured with a balancing hole, which is drilled into the hub plate. It is beneficial during start-up of the pump to relieve the bearing from axial thrust. Since a previous study at nominal rotational speed has already shown, that the distribution of the accumulated gas holdup inside the impeller chambers can be influenced by such a balancing hole (Schäfer et al., 2015), this effect was investigated in more detail. Therefore, the gas holdup profiles in the impeller chambers are analyzed along selected streamlines. These selected streamlines are illustrated as colored lines on the right hand side in Figure 6~~Figure 6~~ and Figure 7~~Figure 7~~. The associated discrete quantitative gas phase fraction values, based on the reconstructed tomographic images, were weighted according to their affiliation to the streamline and assigned to the gas holdup profiles along these selected streamlines. The obtained gas holdup profiles are represented for gas entrainment by swirling two-phase flow for $\varepsilon_{in} = 0.03$ and for an impeller revolution of 1900 rpm in the diagrams in Figure 6~~Figure 6~~ and Figure 7~~Figure 7~~. While Figure 6~~Figure 6~~ represents the profiles of a chamber without a balancing hole, Figure 7~~Figure 7~~ shows the profiles of a chamber equipped with such a balancing hole. The profiles of the impeller chamber without a balancing hole (Figure 6~~Figure 6~~) disclose a slight higher gas holdup in the inner area of the impeller (normalized radii between 0.4 and 0.7) along the central and suction side streamlines than along the pressure-side streamline. But, the gas holdup profiles of the impeller chamber, equipped with a balancing hole (Figure 7~~Figure 7~~), show a completely different behavior. Here, the gas holdup in the inner impeller area along the central and suction side streamlines is much smaller than along the pressure-side streamline. This indicates that the back flow from the pressure side of the hub plate through the balancing hole into the inlet of the corresponding impeller chamber displaces the common path of the incoming flow, which prevents the phase separation and accumulation of a steady gas pocket and, thus, leads to a smaller gas holdup along the central and suction-side area of this chamber. Only the gas holdup along the pressure-side streamline is nearly similar compared to the chamber without a balancing hole. The observed results illustrate the positive impact of the balancing hole, which reduces the phase separation and the accumulation of gas inside the inner area of the impeller. Furthermore, along all selected streamlines and in both impeller chambers a concordant gas holdup value can be discovered at a normalized radius of about 0.7 (transition zone). This indicates an almost homogeneous gas holdup distribution in tangential direction, between

the blades, at this radial position. Here, also a strong reduction of gas accumulation in radial direction, from the inner impeller area to the outer one, takes place. Consequently, this nearly homogeneous local gas holdup distribution in this area indicates that a part of the accumulated gas in the impeller chamber relocates, cross to the liquid flow direction, from the suction-side to the pressure-side, before it is discharged from the impeller chamber. The resulting gas-liquid phase mixing leads to a homogenization of the two-phase flow, which is beneficial for the energy transfer to the liquid and the conveying of the present two phase flow.

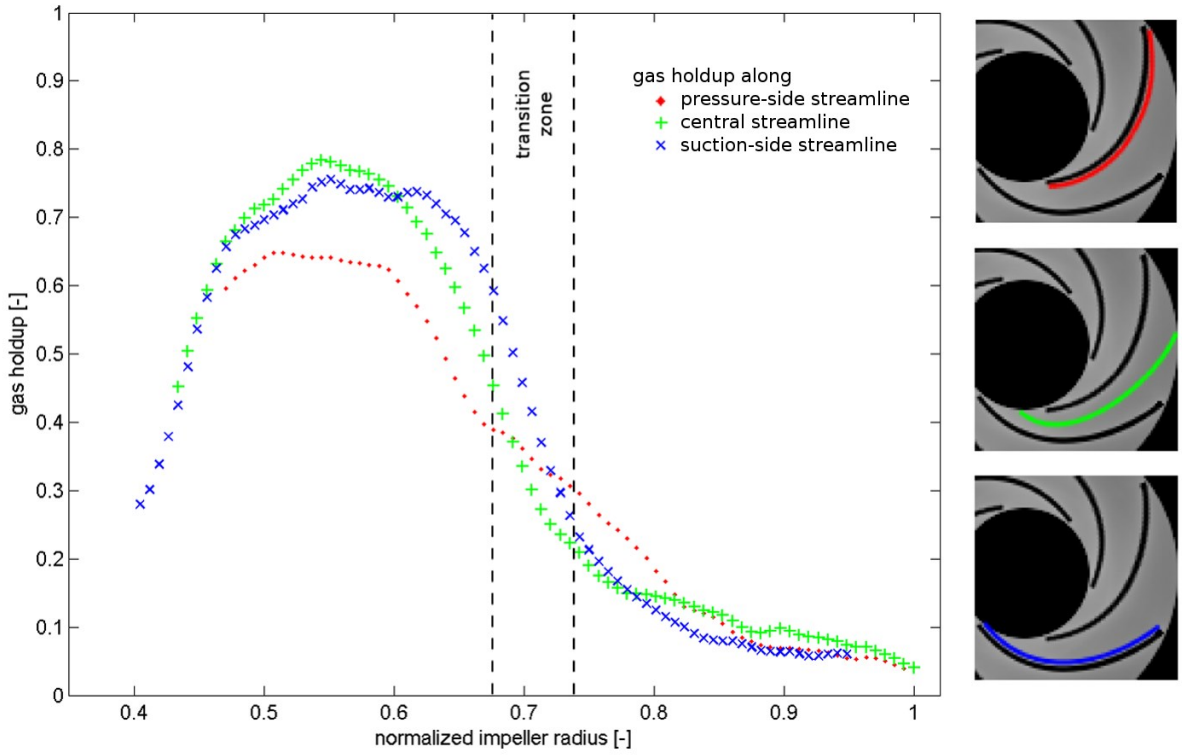

Figure 6: Observed gas holdup profiles along selected streamlines inside an impeller chamber without balancing hole.

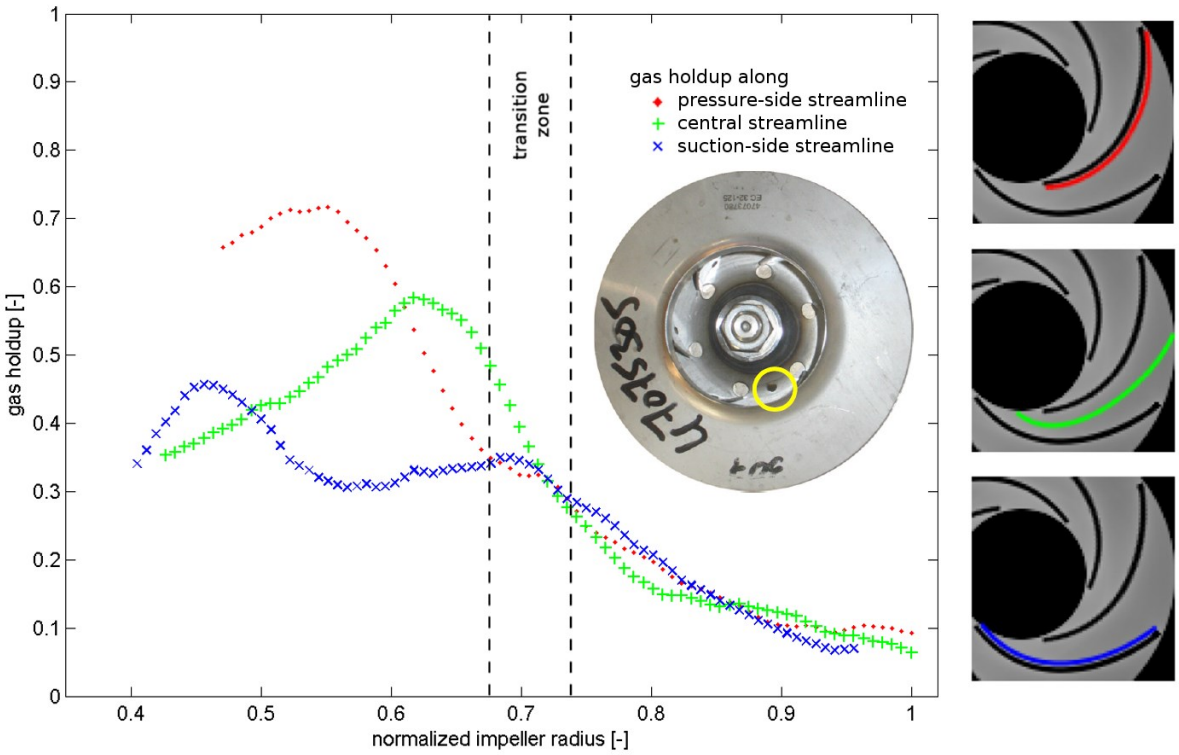

Figure 7: Effect of a balancing hole on the gas holdup inside the corresponding impeller chamber.

4. Conclusion

In this study the effects of gas entrainment in centrifugal pumps, designed for conveying liquids only, have been experimentally investigated. Depending on different gas entrainment conditions, the impact on the hydraulic power of the pump has been analyzed and the influence of the pump installation position has been investigated. It has been discovered, that the gas entraining two-phase flow regime has a large impact on the pump performance. Gas entrainment by swirling two-phase flow regime has been found as more unfavorable compared to gas entrainment by bubbly two-phase flow, since it leads to a higher and discontinuous performance drop. But, regarding to the alignment of the pump no significant impact on the pump performance has been observed. However, for gas entrainment by swirling two-phase flow regime, a vertical impeller alignment leads to a slightly delayed discontinuous performance drop. Additionally, high-resolution gamma-ray computed tomography (HireCT), operated in time-averaged rotation-synchronized scanning mode, has been used to observe and quantify local gas-liquid phase fraction distributions inside the operating pump impeller. Based on these quantitative tomographic measurements, gas holdup profiles in different radially arranged impeller areas and along selected streamlines

have been calculated and analyzed. Thus, structures of gas accumulation inside the impeller chambers have been detected and the impact of a balancing hole on the gas phase accumulation inside the corresponding impeller chamber has been disclosed.

Acknowledgment

The Project is founded by the German Federal Ministry of Education and Research (BMBF) under the funding code 02NUK023B.

References

Bieberle, A.; Schleicher, E.; Hampel, U., **2007**. Data acquisition system for angle synchronized gamma-ray tomography of rapidly rotating objects. *Measurement Science and Technology* 18 (11) pp. 3384-3390.

Bieberle, A.; Berger, R.; Yadav, R.; Schleicher, E.; Hampel, U. **2012**. Design of a modular signal processing board (MSPB) for gamma-ray imaging applications. *Nuclear Instruments and Methods in Physics Research A* 663 (1) pp. 14 - 21.

Bieberle, A.; Nehring, H.; Berger, R.; Arlit, M.; Härting, H.-U.; Schubert, M.; Hampel, U., **2013**. Compact high-resolution gamma-ray computed tomography system for multiphase flow studies. *Review of Scientific Instruments* 84 pp. 033106/1-033106/10.

Bieberle, A.; Schäfer, T.; Neumann, M.; Hampel, U., **2015**. Validation of high-resolution gamma-ray computed tomography for quantitative gas holdup measurements in centrifugal pumps. *Measurement Science and Technology* 26 (9) pp. 1-12.

Caridad, J.; Asuaje, M.; Kenyery, F.; Tremante, A.; Aguillón, O., **2008**. Characterization of a centrifugal pump impeller under two-phase flow conditions. *Journal of Petroleum Science and Engineering* 63 (1-4) pp. 18-22.

Caruso, G., Cristofano, L., Nobili, M., Vitale Di Maio, D., **2014**. Experimental investigation of free surface vortices and definition of gas entrainment occurrence maps. *Journal of Physics* 501 (012019) pp. 1-10.

Chan, A.M.C.; Kawaji, M.; Nakamura, H.; Kukita, Y., **1999**. Experimental study of two-phase pump performance using a full size nuclear reactor pump. *Nuclear Engineering and Design* 193 pp.159-172.

Coutier-Delgosha, O.; Fortes-Patella, R.; Rebound, J.L.; Hofmann, M.; Stoffel, B., **2003**. Experimental and numerical studies in a centrifugal pump with two-dimensional curved blades in cavitating condition. *Journal of Fluids Engineering* 125 pp. 970-977.

398 Duplaa, S.; Coutier-Delgosha, O.; Dazin, A.; Bois, G., **2013**. X-Ray measurements in a
399 cavitating centrifugal pump during fast start-ups. *Journal of Fluids Engineering* 135 pp.
400 041204/1-041204/9.
401 Gonzalez, J.; Santolaria, C., **2006**. Unsteady flow structure and global variables in a
402 centrifugal pump. *Journal of Fluids Engineering* 128 pp. 937-946.
403 Gordon, R.; Bender, R.; Herman, G.T., **1970**. Algebraic Reconstruction Techniques (ART) for
404 three-dimensional Electron Microscopy and X-ray Photography. *J. Theor. Biol.* 29 pp.
405 471-481.
406 Grapsas, A.V.; Anagnostopoulos, J.S.; Papantonis, D.E., **2007**. Experimental and numerical
407 study of a radial flow pump impeller with 2D-curved blades. *Proceedings of the 5th*
408 *IASME/WSEAS International Conference on Fluid Mechanics and Aerodynamics* Athens
409 Greece August 25-27.
410 Hampel, U.; Hoppe, D.; Diele, K.-H.; Fietz, J.; Hoeller, H.; Kernchen, R.; Prasser, H.-M.;
411 Zippe, C., **2005**. Application of gamma tomography to the measurement of fluid
412 distributions in a hydrodynamic coupling. *Flow Measurement and Instrumentation* 16
413 pp. 85-90.
414 Hampel, U.; Bieberle, A.; Hoppe, D.; Kronenberg, J.; Schleicher, E.; Suehnel, T.;
415 Zimmermann, W.; Zippe, C., **2007**. High resolution gamma ray tomography scanner for
416 flow measurement and non-destructive testing applications. *Review of Scientific*
417 *Instruments* 78 (10) p. 103704.
418 Hampel, U.; Hoppe, D.; Bieberle, A.; Kernchen, R.; Diele, K.-H.; Schleicher, E.; Da Silva, M. J.;
419 Zippe, C., **2008**. Measurement of fluid distributions in a rotating fluid coupling using
420 high resolution gamma ray tomography. *Journal of Fluids Engineering - Transactions on*
421 *ASME*, 130 (9) p. 091402.
422 Hecker, G.E., **1981**. Model-prototype comparison of free surface vortices. *Journal of the*
423 *Hydraulics Division* ASCE, 107 pp. 1243-1259.
424 Kimura, N., Ezure, T., Tobita, A., Kamide, H., **2008**. Experimental study on gas entrainment at
425 free surface in reactor vessel of a compact sodium-cooled fast reactor. *Journal of*
426 *Nuclear Science and Technology* 45 (10) pp. 1053-1062.
427 Narabayashi, T.; Arai, K.;Kubokoya, T.; Amano, O.; Gomyo, T., **1985**. Centrifugal pump
428 behavior in steady and transient two-phase flow. *Journal of Nuclear Science and*
429 *Technology* 23 (2) pp. 136-150.

Neumann, M.; Schäfer, T.; Bieberle, A.; Hampel, U., forthcoming **2016**. An experimental study on the gas entrainment in horizontally and vertically installed centrifugal pumps. *Journal of Fluids Engineering* doi: 10.1115/1.4033029.

Pak, E.T.; Lee, J.C., **1998**. Performance and pressure distribution changes in a centrifugal pump under two-phase flow. *Proc. Inst. Mech. Eng.* 212 pp. 165-171.

Prasser, H.-M.; Baldauf, D; Fietz, J.; Hampel, U.; Zippe, C.; Zschau, J.; Christen, M.; Will, G., **2003**. Time resolving gamma-tomography for periodically changing gas fraction fields and its application to an axial pump. *Flow Measurement and Instrumentation* 14 pp. 119-125.

Schäfer, T.; Bieberle, A.; Neumann, M.; Hampel, U., **2015**. Application of gamma-ray computed tomography for the analysis of gas holdup distributions in centrifugal pumps. *Flow Measurement and Instrumentation* 46 pp. 262-267.

Schubert, M.; Bieberle, A.; Barthel, F.; Boden, S.; Hampel, U., **2011**. Advanced tomographic techniques for flow imaging in columns with flow distribution packings. *Chemie Ingenieur Technik* 83 (7) pp. 979-991.

Suhane, A., **2012**. Experimental study on centrifugal pump to determine the effect of radial clearance on pressure pulsations vibrations and noise. *International Journal of Engineering Research and Applications* 2 (4) pp. 1823-1829.

Tan, L.; Zhu, B.S.; Cao, S.L.; Wang, Y.M., **2013**. Cavitation flow simulation for a centrifugal pump at low flow rate. *Chinese Science Bulletin* 58 (8) pp. 949-952.

Zhang, Y.; Zuchao, Z.; Jin, Y.; Cui, B.; Li, Y.; Dou, H., **2013**. Experimental study on a centrifugal pump with open impeller during start-up period. *Journal of Thermal Science* 22 (1) pp. 1-6.

Zhou, L.; Shi, W.; Wu, S., **2013**. Performance optimization in a centrifugal pump impeller by orthogonal experiment and numerical simulation. *Advances in Mechanical Engineering* 2013 (385809) pp. 1-7.